Per- and polyfluoroalkyl substances (PFAS) in surface sediments: occurrence, patterns, spatial distribution and contribution of unattributed precursors in French aquatic environments

Nicolas Macorps[1], Pierre Labadie[1]*, François Lestremau[2,3], Azziz Assoumani[2], Hélène Budzinski[1]

[1] CNRS/Université de Bordeaux, UMR 5805 EPOC, Talence, France

[2] INERIS, Unité Méthodes et développements en Analyses pour l'Environnement, 60550 Verneuil-en-Halatte, France

[3] now at Hydrosciences Montpellier, Univ. Montpellier, IMT Mines Ales, IRD, CNRS, Ales, France

*contact pierre.labadie@u-bordeaux.fr

Abstract

While perfluoroalkyl sulfonic acids (PFSAs) and perfluoroalkyl carboxylic acids (PFCAs) are ubiquitous in aquatic environments, non-targeted methods have recently revealed the presence of numerous unidentified per- and polyfluoroalkyl substances (PFAS). Besides those methods, the total oxidizable precursor (TOP) assay has proved useful to estimate the contribution of unattributed perfluoroalkyl acids precursors (pre-PFAAs). In this study, an optimized extraction method was developed to examine the spatial distribution of 36 targeted PFAS in surface sediments collected at French nationwide scale

(n = 43), including neutral, anionic and zwitterionic molecules. In addition, a TOP assay procedure was implemented to estimate the contribution of unattributed pre-PFAAs in these samples. Conversion yields of targeted pre-PFAAs were determined for the first time under realistic conditions and led to differences in oxidation profiles compared to the common spiked ultra-pure water method. PFAS were detected in 86% of samples and $\sum PFAS_{targeted}$ was in the range <Limit of Detection – 23 ng g^{-1} dry weight (dw) (median: 1.3 ng g^{-1} dw), with $\sum pre\text{-}PFAAs_{targeted}$ representing on average 29 ± 26 % of $\sum PFAS$. Among pre-PFAAs, compounds of emerging interest such as the fluorotelomer sulfonamidoalkyl betaines 6:2 FTAB and 8:2 FTAB were respectively detected in 38% and 24% of samples, with levels similar to those of L-PFOS (<0.36 – 2.2, <0.50 – 6.8 and <0.08 – 5.1 ng g^{-1} dw, respectively). A hierarchical cluster analysis coupled with a geographic information system-based approach revealed similarities between groups of sampling sites. For instance, elevated contribution of FTABs were associated with the proximity to airport activities where betaine-based aqueous film-forming foam (AFFFs) might have been used. In addition, unattributed pre-PFAAs were strongly correlated with $\sum PFAS_{targeted}$ and they accounted for 58% of $\sum PFAS$ (median value); they were generally found in larger quantity near industrial and urban areas where the highest $\sum PFAS_{targeted}$ were also observed.

Highlights

- Emerging PFAS were widely distributed (e.g. 6:2 FTAB detected in 37.8 % of samples)

- Peculiar molecular patterns were found near industrial and airport areas

- The TOP assay was adapted for sediments under realistic conditions

- Elevated amounts of unattributed PFAA precursors were reported at nationwide scale

1. Introduction

Per- and polyfluoroalkyl substances (PFAS) have been extensively used since the 1950s in numerous industrial applications such as in the fluoropolymer industry, domestic products or aqueous film-forming foams (AFFFs) (Buck et al. 2011; Glüge et al. 2020). They are of major environmental concern because of their persistence, bioaccumulative properties and toxicity (Ahrens 2011). The worldwide presence in aquatic environments of perfluoroalkyl acids (PFAAs), in particular perfluoroalkyl carboxylates (PFCAs) and perfluoroalkyl sulfonic acids (PFSAs), has been substantially reported (Ahrens 2011; Houde et al. 2011; Zareitalabad et al. 2013; Pan et al. 2018). Perfluorooctane carboxylate (PFOA), perfluorooctane sulfonate (PFOS) and their salts have been listed under Annex B and A of the Stockholm Convention (Wang et al. 2017). The latter is also listed as a priority pollutant under the Water Framework Directive (WFD) since 2013 (European Commission 2013). As a consequence of PFAS regulation, a shift towards alternative PFAS was initiated in recent years, leading to the phase-out of long-chain compounds and to the increased detection of emerging compounds (Xiao 2017), such as zwitterionic PFAS (*e.g.* 6:2 fluorotelomer sulfonamidoalkyl betaine (6:2 FTAB)).

Over 4700 PFAS are or have been released on the market, with less than 6% being commercially relevant (Cousins et al. 2020). However, the lack of analytical standards and instrument limitations has led to the quantitative monitoring of a limited number of PFAS only (Ruan and Jiang 2017). Applications of other analytical methods such as total/extractible organic fluorine measurements (Yeung et al. 2013) or the total oxidizable precursor assay (TOP) (Houtz and Sedlak 2012) proved useful to account for the non-targeted PFAS fractions (Cousins et al. 2020). For instance, the TOP assay, which relies on the oxidative conversion of perfluoroalkyl precursors (pre-PFAAs) into PFCAs, highlighted that unattributed pre-PFAAs contributed for 80% of ∑PFAS in urban sediments (Simonnet-Laprade et al. 2019). Large fractions of unattributed pre-PFAAs were also found in other environments, *e.g.* urban runoff, groundwater and urban rivers (Houtz and Sedlak 2012; Houtz et al. 2013; Ye et al. 2014; Boiteux et al. 2017), but studies remained limited to local and regional scales. Only few studies have explored

TOP assay application in sediments, soil or suspended particulate matter (Göckener et al. 2022; Guckert et al. 2022; Liu et al. 2022). This promising method is not standardized yet (Cousins et al. 2020) and it still requires development, especially for solid and complex matrices with organic residues (Casson and Chiang 2018).

Recent findings on emerging PFAS in aquatic environment were reviewed by Xiao (2017). The numerous newly reported PFAS include but are not limited to the following compounds: perfluoroether sulfonic acids (PFESAs) and carboxylic acids (PFECAs) such as 6:2 chlorinated polyfluorinated ether sulfonic acid (6:2 Cl-PFESA), mostly used in electroplating industry in China (Wang et al. 2013), hexafluoropropylene oxide-dimer acid (HFPO-DA) and dodecafluoro-3H-4,8-dioxanonanoate (ADONA), *i.e.* PFOA replacement in fluoropolymer industry (Munoz et al. 2019) or PFECHS, found in hydraulic fluids (De Silva et al. 2011). In addition, 6:2 FTAB, found in the betaine-based AFFFs used in firefighting activities (Dauchy et al. 2017), has been internationally reported near AFFF-impacted sites (D'Agostino and Mabury 2017; Munoz et al. 2017; Chen et al. 2020). To further characterize the environmental occurrence of these PFAS, there is a need for spatial distribution studies, based on extended lists of targeted compounds with robust and sensitive methods adapted for newly identified PFAS.

In this context, the present work aimed at investigating i) the occurrence and spatial distribution of a large range of targeted PFAS and ii) the contribution of unattributed pre-PFAAs in surface sediments, collected at French nationwide scale. A previous survey, which monitored 22 individual PFAS, highlighted the ubiquity of PFOS and long-chain PFCAs in sediments, with elevated PFAS levels and distinct molecular patterns near industrial and urban areas (Munoz et al. 2015). Here, a method was optimized for the targeted analysis of a much wider range of PFAS (n = 36), combined with an adapted TOP assay procedure. Conversion yields of targeted pre-PFAAs into PFCAs were evaluated for the first time under realistic extraction conditions (*i.e.* in the presence of organic solvent/salt residues) and the procedure was validated on sediments sample extracts. The newly developed methods were

subsequently applied to surface sediments samples (n=43). In addition, the spatial distribution of PFAS and unattributed pre-PFAAs was investigated by combining cluster analysis and a geographic information system (GIS)-based approach.

2. Materials and methods

2.1. Standards and reagents

A total of 36 individual PFAS were targeted, including eleven PFCAs (C_4–C_{14}), five PFSAs ($C_{4,6,7,8,10}$), three perfluoroalkyl sulfonamides (FOSA, N-MeFOSA and N-EtFOSA), three perfluoroalkyl sulfonamides acetic acids (FOSAA, N-MeFOSAA and N-EtFOSAA), four fluorotelomer sulfonates (4:2, 6:2, 8:2 and 10:2 FTSA), two polyfluoroalkyl phosphoric acid diesters (6:2 and 8:2 diPAP), two FTABs (6:2 and 8:2 FTAB), two chlorinated PFESAs (6:2 and 8:2 Cl-PFESA), one cyclic PFESA (PFECHS), one polyfluoroalkyl carboxylate (5:3 FTCA) and two PFECAs (ADONA and HFPO-DA). In this paper, L-PFOS refers to the linear PFOS isomer and Br-PFOS to the sum of branched PFOS isomers. Full details on chemicals, standard solutions and consumables are provided in the supplementary information (SI, Table S1).

2.2. Sampling

To represent the wide variety of environments encountered in French hydrosystems, diverse sampling sites were selected by the French National Institute for Industrial Environment and Risks (INERIS), *i.e.* sites exhibiting "good ecological status" according to the European Union WFD (European Commission 2000) and sites under heavier anthropogenic pressure (*e.g.* close to urban, industrial or agricultural areas). Composite surface sediment samples (0–5 cm depth) were collected during a single sampling campaign (September–November 2018) at 43 sites located in the hydrographic network and in coastal areas (Figure 1). Sampling was undertaken during a low-flow period that i) favored the deposition of fine-grained sediments and ii) minimized sediment remobilization. Samples were stored in a cooling

box (4°C), pending shipment to the laboratory within 24 h. River flow rate data were obtained from Banque Hydro (<www.hydro.eaufrance.fr>). Full details on sampling site names, locations and types of anthropogenic pressure as determined by INERIS and by the GIS approach are given in Table S2.

2.3. Sample preparation and analysis

Upon arrival at the laboratory, sediment able samples were sieved (< 2mm). Two aliquots (15 mL) were taken for the characterization of total organic carbon (TOC) content and the determination of the fine fraction content (*i.e.* silt content, < 63 µm). Sediment samples were freeze-dried, finely grounded with a ball mill (< 250 µm) and stored at room temperature in amber glass jars prior to extraction.

The sample extraction procedure was adapted from a previous study carried out by our group (Simonnet-Laprade et al. 2019). Briefly, sediments (1 g dry weight, dw) were supplemented with internal standards (ISs, 2 ng each) and extracted using microwaved-assisted solvent extraction with 250 mM CH_3COONH_4 in MeOH (12 mL), followed by filtration on glass wool and graphitized carbon clean-up. Extracts were evaporated to approximately 300 µL under a gentle nitrogen stream at 40 °C and stored at -20°C prior to analysis. Procedural blanks consisted of extraction solvent, while spiked controls (i.e. accuracy assessment) consisted of sediment samples spiked with PFAS (i.e. in-house reference material); in both cases, ISs were added at the beginning of the procedure.

Targeted PFAS analysis was performed using liquid chromatography electrospray ionization coupled with tandem mass spectrometry (LC-ESI-MS/MS) on a 1290 LC system interfaced with a 6495 triple quadrupole mass spectrometer (Agilent Technologies, Massy, France). Due to the inclusion of FTABs in this work, the ESI source was set on fast polarity switching mode. Further details are provided in the SI (Table S3 and Table S4).

2.4. Total oxidizable precursor (TOP) assay

The sediment extract oxidation procedure was adapted from Simonnet-Laprade et al. (2019) with some modifications. Sediments (0.2 g) were first extracted and cleaned up as described above for targeted analysis. Extracts were then reduced to approximately 100 µL, transferred into 125 mL HDPE bottles and evaporated to dryness at room temperature under a nitrogen stream. Next, 100 mL of ultra-pure water amended with 200 mM $K_2S_2O_8$ and 500 mM NaOH were added to the bottles, followed by sonication (20 min) to assist PFAS dissolution. Extracts were incubated at 85°C for 6h, then cooled down and neutralized with HCl (3M) (i.e. 1–2 mL). To prevent their oxidation, ISs (4 ng each) were added at this stage. Samples were subsequently extracted on Strata X-AW cartridges and analyzed with LC-ESI-MS/MS. Oxidation procedural blanks consisted of extraction solvent that was submitted to the TOP assay as described for sediment sample extracts.

The conversion rates of targeted precursors into PFCAs upon oxidation (Table S5) were determined on spiked extraction solvent (n = 5), *i.e.* 12 mL of MeOH + 250 mM CH_3COONH_4 concentrated to approximately 100 µL. TOP assay data were used i) to calculate the increase of ∑PFCAs (termed ΔPFCAs hereafter and expressed on a molar basis) and ii) to estimate the total extractable amount of ∑pre-PFAAs (herein termed ∑pre-PFAAs$_{total}$). Conversion rates were used to determine the fraction of ΔPFCAs resulting from the oxidation of targeted pre-PFAAs that, in turn, allowed for the estimation of PFCA amounts resulting from the oxidation of unattributed pre-PFAAs (∑pre-PFAAs$_{unattributed}$).

Oxidation performances in the presence of matrix residues were assessed through the triplicate analysis of two sediments with contrasted TOC content. Details on conversion rate determination, oxidation performances on sediments and calculations are provided in the "TOP assay" section of the SI.

2.5. Quality control

For analytes quantified in procedural blanks (Table S6), data were blank-corrected and limits of detection (LODs) were either based on blanks or on signal-to-noise as described elsewhere (Simonnet-Laprade et al. 2019). LODs were in the range 0.006–0.78 ng g^{-1} dw (Table 1) and limits of quantification (LOQs) were determined as 10/3*LODs.

As regards targeted analyses, whole method recoveries for spiked sediments were in the range 80–120% except for 6:2 FTAB and 8:2 FTAB (67% and 62%, respectively) and relative standard deviations (RSD) remained generally below 20% except for FTSAs (21–26%) (Table S7). Accuracy was determined with sediments spiked with ISs and analytes at the beginning of the procedure (1 ng g^{-1} each); values were in the range 80–120% except for 6:2 FTAB, 8:2 FTAB, 8:2 diPAP and PFBS (60%, 58%, 122% and 122%, respectively). TOP assay validation details are given in the "TOP assay" section of the SI.

2.6. Statistics

The R statistical software (R version 4.0.5, R core team 2021) was used to perform statistical analyses. To account for non-detects (*i.e.* < LOD), descriptive statistics, correlations and differences between groups were calculated using functions from the *NADA-R* package (Munoz et al. 2015). Descriptive statistics for compounds with > 80% non-detected values were not computed and were reported as "NC" (not calculated) (Helsel, 2011). Hierarchical cluster analysis based on Ward's minimum variance classification and Euclidian distance between variables (break-in set at 4 clusters) was computed with the *FactoMiner* package (function *hclust*) for R. Details on the GIS method are provided in the SI (section "GIS approach").
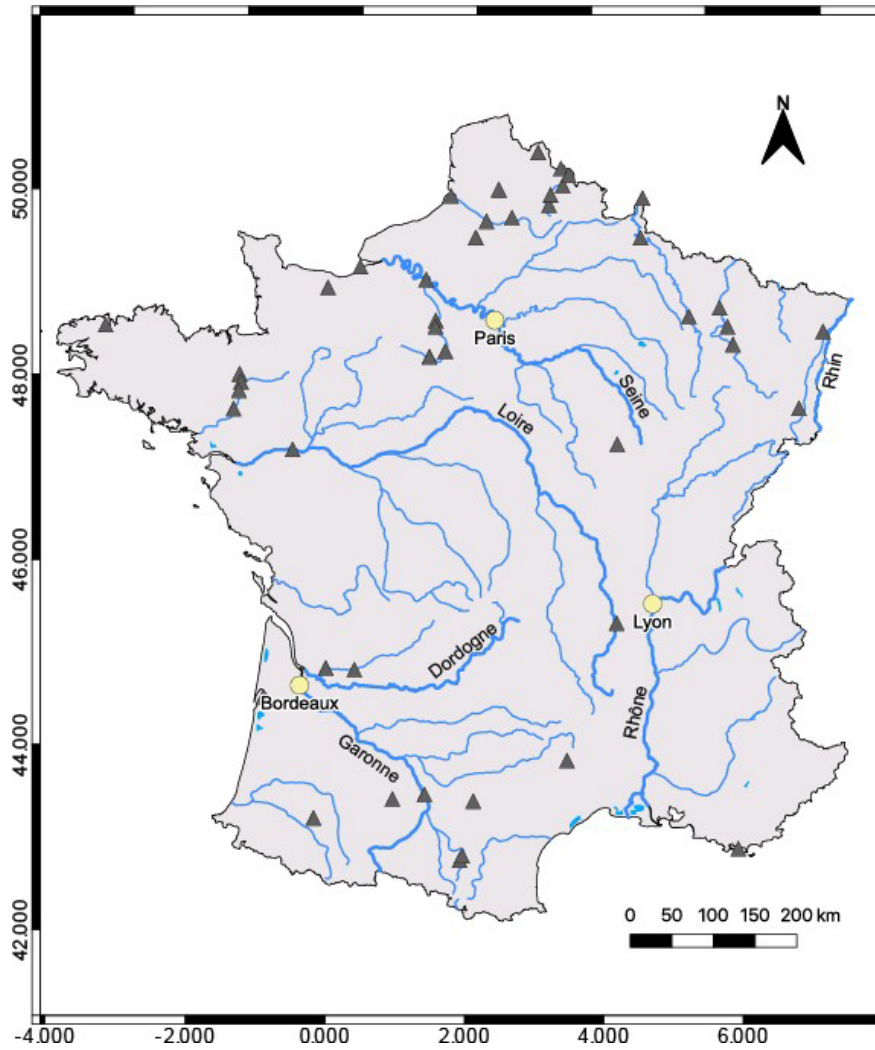
Figure 1. Map showing the 43 sampling sites.

3. Results and discussion

3.1. Optimization of extraction and TOP methods

Due to the inclusion of FTABs in the list of targeted PFAS, the method from Munoz et al. (2015) had to be adapted (*i.e.* extraction solvent). Preliminary results revealed that when using MeOH + 0.2% NH$_4$OH as extraction solvent, low recovery yields were achieved for zwitterionic analytes (c.a. 30 %) (Figure S4). However, the addition of ammonium acetate (250 mM) to MeOH dramatically improved FTAB recoveries (> 60%); this solvent also proved suitable for the extraction of the other classes of PFAS targeted in this work (i.e. recoveries in the range 80–110%). Such improvement in the extraction of FTABs and several other unfrequently reported PFAS classes has previously been documented on soils (Munoz et al. 2018) but it is reported here for the first time for sediments.

The TOP assay procedure was adapted based on the new extraction method. Assessment of molar conversion yields of targeted pre-PFAAs was conducted in ultra-pure water and in spiked extraction solvent. Using concentrations of 150 mM NaOH and 60 mM potassium persulfate (Houtz and Sedlak 2012; Simonnet-Laprade et al. 2019), incomplete conversions were observed in spiked solvent samples (data not shown). Reagent concentrations were increased to 500 mM NaOH and 200 mM potassium persulfate and complete conversion of the tested pre-PFAAs was achieved, except for 8:2 FTSA and 10:2 FTSA (remaining fractions < 10%) (Table S5). Conversion yields of targeted pre-PFAAs were, however, different between the two conditions. In ultra-pure water, N-MeFOSAA was near-quantitatively converted to PFOA with C$_5$–C$_7$ PFCAs as minor oxidation products, in good agreement with the literature (Martin et al. 2019; Simonnet-Laprade et al. 2019). Conversely, when tests were performed on spiked solvent, a mixture of C$_4$–C$_8$ PFCAs was generated (Table S5), with good reproducibility. All tested pre-PFAAs displayed similar trends. The increase in reagent concentrations may alter oxidation profiles towards shorter PFCAs (Göckener et al. 2020; Liu et al. 2021), which requires specific analytical methods (Janda et al. 2019; Martin et al. 2019). Hence, incomplete mass balance was achieved and, consequently, ΔPFCAs and ∑pre-PFAAs$_{unattributed}$ reported thereafter should

be viewed as low estimates. However, it should be emphasized that we conducted conversion experiments under conditions similar to those used for samples (*i.e.* in the presence of solvent and salt residues). This point has, to the authors' knowledge, never been investigated for the application of the TOP assay to sediments and previous results published in the literature may therefore have been biased. It is noteworthy that the complete conversion of pre-PFAAs$_{targeted}$ was observed when the TOP assay was applied on sediments samples with contrasted TOC contents (Figure S3), which illustrates the robustness of the procedure. Overall, the optimized extraction step improved the recovery of target pre-PFAAs belonging to different PFAS groups with very different chemistries. It is therefore reasonable to assume that this procedure also enhanced the recovery of unattributed precursors, thereby increasing the relevance of the TOP assay performed under such conditions.

3.2. Targeted analysis

3.2.1. Detection frequency and levels

Overall, PFAS were detected in 86 % of sediment samples (Table 1). L-PFOS, PFDoDA and PFOA were the most detected compounds (detection frequency: 75%, 71% and 71%, respectively) with median concentrations of 0.44, 0.13 and 0.07 ng g^{-1} dw, respectively. Emerging PFAS such as HFPO-DA, ADONA, 6:2 Cl-PFESA and 8:2 Cl-PFESA were not detected in the samples analyzed in this work, suggesting the current lower use and emission of these compounds on the French territory compared to other parts of the world (Pan et al. 2018; Chen et al. 2020). The infrequently reported 6:2 FTAB, 10:2 FTSA and 5:3 FTCA were detected in > 35% of samples, while 8:2 FTAB was less often detected (detection frequency: 24.4 %); for all these compounds, the median concentration was lower than the LOD.

The median concentration of ∑PFAS was 1.3 ng g^{-1} dw, which is larger than in a previous French nationwide survey performed in 2012 (0.48 ng g^{-1} dw) (Munoz et al. 2015). However, it should be kept in mind that i) a larger list of PFAS was targeted in this study, including 6:2 FTAB and 8:2 FTAB that

were found in the ng g^{-1} range, and ii) sampling sites were different. High levels of FTABs have been reported near point sources (Boiteux et al. 2016; Munoz et al. 2017; Chen et al. 2020; Meng et al. 2021). Such compounds were previously semi-quantified through suspect screening analysis on a limited number of samples (n = 12 / 129) from the 2012 survey (Munoz et al. 2016) ; their presence in French aquatic environment at similar levels than L-PFOS was therefore confirmed in this study at large spatial scale, advocating for their inclusion in targeted analysis lists.

3.2.2. Molecular patterns and spatial distribution

L-PFOS was the prevalent compound, i.e. accounting for 38% of ∑PFAS$_{targeted}$ on average, in agreement with previous studies (Hloušková et al. 2014; Munoz et al. 2015; Pignotti et al. 2017). It was followed by 6:2 FTAB and PFDoDA (11% and 10% respectively) (Table S8). Overall, ∑pre-PFAAs$_{targeted}$ was variable and represented on average 29 ± 26 % of ∑PFAS$_{targeted}$; 6:2 FTAB and 8:2 FTAB accounted for a large fraction of ∑pre-PFAAs$_{targeted}$ (21 ± 29% and 13 ± 23%, respectively) (Figure S5), which is consistent with other studies (Chen et al. 2020; Meng et al. 2021). When detected, 5:3 FTCA represented 2–14% of ∑PFAS, suggesting that significant biotransformation of fluorotelomer-based products such as fluorotelomer alcohol or FTSAs may have occurred at some sites (Butt et al. 2014).

The most contaminated site was located on the Canal de la Deûle (St0112), a few km downstream from the Lille conurbation (> 1 M inhabitants). At this site, ∑PFAS reached 23 ng g^{-1} dw, of which 45% was due to ∑pre-PFAAs$_{targeted}$. Out of the fourteen targeted pre-PFAAs, eleven were detected at this site with elevated levels of N-MeFOSAA (2.5 ng g^{-1} dw) and ∑FTABs (4.9 ng g^{-1} dw). FOSA, EtFOSAA and 6:2 FTSA, also detected at this site, are known products of the transformation of fluorotelomer-based PFAS (such as 6:2 FTAB) and perfluoroalkane sulfonamido derivatives (FASAs) (Liu and Mejia Avendaño 2013; D'Agostino and Mabury 2017). The Deûle River is characterized by a low water flow rate (mean < 10 m^3 s^{-1} over the 2005-2010 period) and the sampling site was located i) downstream of a large

wastewater treatment plant (WWTP) with a nominal capacity of 620 000 population equivalent and ii) 15 km downstream from the Lille-Lesquin International Airport. Higher number of emerging PFAS and higher PFAS concentration were generally observed near urban center and large WWTP (Munoz et al. 2016; Chen et al. 2020; Ali et al. 2021). Thus, the small dilution capacity of the river combined with large PFAS inputs near the sampling site may likely explain the large fraction of $\sum$pre-PFAAs$_{targeted}$ as well as the relatively high L-PFOS concentration (5.1 ng g^{-1} dw).

In order to highlight similarities in PFAS patterns between sites, a hierarchical ascendant classification (HAC) was performed for sampling sites where at least one PFAS was detected. For the sake of HAC interpretation in relation with site typology, we have arbitrarily set the break-in at 4 clusters. This resulted in clusters comprising 12, 1, 15 and 11 sites (Figure 2). No regional effect could be observed in the HAC since sites from different basins were distributed in the different clusters (*i.e.* the major driver of clustering was land use/human activities rather than geographical location). Cluster #01 grouped sites with low contamination levels (i.e. $\sum$PFAS < ng g^{-1} dw) where almost 100% of $\sum$PFAS (*i.e.* > 97 %) could be attributed to $\sum$PFCAs + $\sum$PFSAs. These sites were generally distant or upstream from major urban centers and they may be mainly contaminated by diffuse inputs such as atmospheric deposition (Ahrens 2011). Cluster #02 was represented by a single site (St0516) that exhibited high levels of both $\sum$FTABs (8.4 ng g^{-1} dw), accounting for 62% of $\sum$PFAS, and 6:2 diPAP (1.5 ng g^{-1} dw, 11% of $\sum$PFAS). This site was located on a small river with a low water flow rate (mean < 1 m^3 s^{-1} over the 2009 – 2020 period) and < 10km from the Toulouse-Blagnac airport where fire-fighting activities involving betaine-based AFFFs may occur on a regular basis (Place and Field 2012). Clusters #03 and #04 differed from #01 mainly because of their relative contributions of individual pre-PFAAs to $\sum$pre-PFAAs$_{targeted}$. Sites associated with Cluster#03 showed $\sum$PFAS ranging from 1.0 up to 23 ng g^{-1} dw with a contribution of $\sum$pre-PFAAs$_{targeted}$ to $\sum$PFAS mostly dominated by 6:2 FTAB and 8:2 FTAB. Most of the sites from Cluster#03 were located close to large urban centers and influenced by nearby airport activities. Finally, sampling sites belonging to cluster #04 showed a different pre-PFAAs pattern, *i.e.* $\sum$pre-PFAAs$_{targeted}$ was dominated by FTSAs and PFOS precursors (e.g. N-MeFOSAA and N-EtFOSAA) ;

they were mainly impacted by industrial activities and close to medium size cities (<150 000 habitants). Although FTSAs and PFOS precursors were proposed as degradation intermediates from fluorotelomers-based products such as FTABs (D'Agostino and Mabury 2017), peculiar molecular patterns characterized by a large relative contribution of 6:2 FTSA are consistent with sampling sites under industrial pressure (Munoz et al. 2015; Chen et al. 2020). Finally, coastal sediments (n = 4) showed $\sum$PFAS in the range <LOD – 1.0 ng g^{-1} dw, with no distinct molecular pattern.

Given the size of the dataset and the variety in anthropogenic pressure on the different sites, the hierarchical ascendant classification and GIS approach proved useful to highlight specific molecular patterns and identify probable PFAS sources.

3.3. Correlations

C_8–C_{14} PFCAs were correlated with each other (Table S9) as well as with L-PFOS, Br-PFOS, FOSA, 10:2 FTSA, FTABs and 5:3 FTCA, which strongly suggests similar sources or fate. N-MeFOSAA was not correlated with FTABs nor 5:3 FTCA, which could be linked to the fact that N-MeFOSAA was not identified as a degradation product of FTABs (Shaw et al. 2019), but rather as a PFOS precursor (Buck et al. 2011). Since 5:3 FTCA was found to be a degradation product of FTABs and FTSAs (Zhang et al. 2016; Shaw et al. 2019), the correlation between 5:3 FTCA levels and $\sum$FTSAs + $\sum$FTABs levels was tested. This correlation was highly significant (slope = 26.4, Kendall's τ = 0.48, $p < 0.001$); this also suggests that, along with FTSAs and FTABs, other PFAS not targeted in this work may also contribute to the 5:3 FTCA burden in sediments.

Sediment characteristics such as TOC or silt content were found to be relevant controlling factor of PFAS sediment-water partition coefficients, with TOC content being more influential (Munoz et al. 2015). Here, the correlation between PFAS levels in sediments and TOC were tested for both legacy PFAAs (considered as benchmark compounds) and for the emerging PFAS most frequently detected

(i.e. in > 20 % of samples): 10:2 FTSA, 6:2 FTAB, 8:2 FTAB, and 5:3 FTCA. Significant correlations were found for both legacy and emerging PFAS, except N-MeFOSAA (Table S10). However, Kendall's τ remained relatively low, which might for instance suggest that the interaction with organic carbon is not the only mechanism playing a role in PFAS sorption (Barzen-Hanson et al. 2017; Xiao et al. 2019).

Table 1. PFAS detection frequency, concentration range and median observed in sediments (n = 43). Median values were computed with the Regression on Order Statistics (robust ROS) approach. NC: not calculated (> 80% non-detects).

	Detection limit (ng g^{-1} dw)	Detection frequency (%)	Range (ng g^{-1} dw)	Median (ng g^{-1} dw)
PFBA	0.43	8.9	<0.43−0.74	NC
PFPeA	0.45	-	-	NC
PFHxA	0.24	4.4	<0.24−1.2	NC
PFHpA	0.04	15.6	<0.04−0.13	NC
PFOA	0.05	71.1	<0.05−0.58	0.07
PFNA	0.03	42.2	<0.03−0.14	<0.03
PFDA	0.06	33.3	<0.06−0.46	<0.06
PFUnDA	0.07	35.6	<0.07−0.44	0.07
PFDoDA	0.05	71.1	<0.05−0.77	0.13
PFTrDA	0.06	28.9	<0.06−1.1	<0.06
PFTeDA	0.06	46.7	<0.06−0.60	<0.06
PFBS	0.03	-	-	NC
PFHxS	0.02	6.7	<0.02−0.16	NC
PFHpS	0.05	-	-	NC
Br-PFOS	0.10	42.2	<0.10−0.87	0.10
L-PFOS	0.08	75.6	<0.08−5.1	0.44
PFDS	0.04	2.2	<0.04−0.26	NC
FOSAA	0.04	13.3	<0.04−0.17	NC
N-MeFOSAA	0.03	28.9	<0.03−2.5	<0.03
N-EtFOSAA	0.03	42.2	<0.03−0.85	0.03
FOSA	0.02	44.4	<0.02−0.11	0.02
N-MeFOSA	0.02	15.6	<0.02−0.26	NC
N-EtFOSA	0.01	11.1	<0.01−0.15	NC
4:2 FTSA	0.02	-	-	NC
6:2 FTSA	0.12	8.9	<0.12−2.1	NC
8:2 FTSA	0.09	15.6	<0.09−1.1	NC
10:2 FTSA	0.10	37.8	<0.10−0.84	<0.10
6:2 diPAP	0.78	2.2	<0.78−1.5	NC
8:2 diPAP	0.71	-	-	NC
6:2 FTAB	0.36	37.8	<0.36−2.2	<0.36
8:2 FTAB	0.50	24.4	<0.50−6.8	<0.50
HFPO-DA	0.05	-	-	NC
ADONA	0.006	-	-	NC
6:2 Cl-PFESA	0.03	-	-	NC
8:2 Cl-PFESA	0.04	-	-	NC
PFECHS	0.04	2.2	<0.04−0.04	NC
5:3 FTCA	0.08	35.6	<0.08−1.8	<0.08
∑PFAS	**-**	**86.7**	**<LOD−23**	**1.3**

1
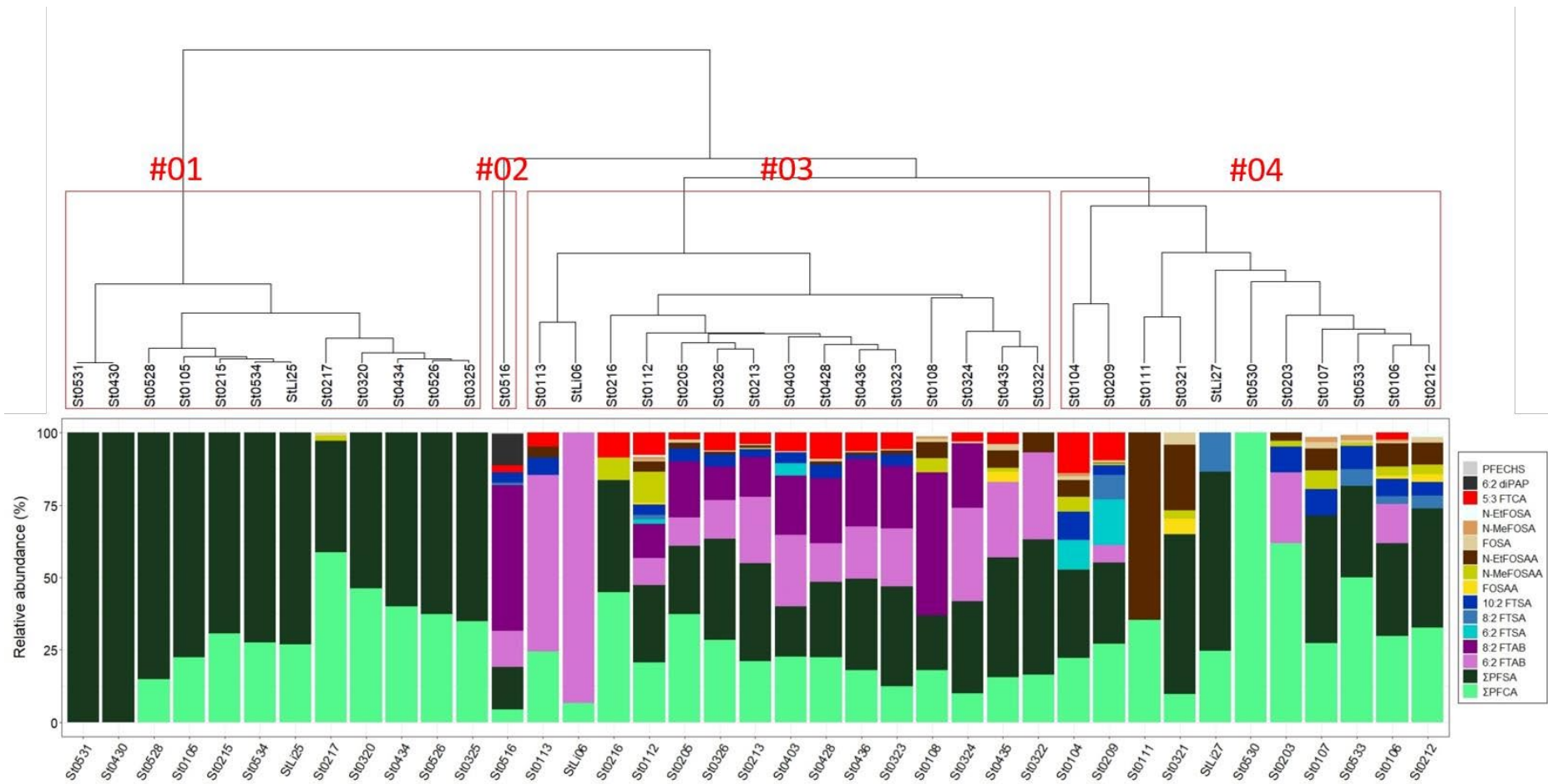
Figure 2. PFAS molecular patterns in sediment arranged through HAC.

3.4. PFAAs precursors as estimated by oxidation

3.4.1. Contribution of unattributed precursors

Data from the TOP assay revealed the presence of unattributed pre-PFAAs in most samples. Upon oxidation, significant ΔPFCAs values were measured (Table S11) in 37 out of 43 samples (*i.e.* 86 %). Five samples that displayed $\sum$PFAS < LOD using targeted analysis showed no significant ΔPFCAs after oxidative treatment. These samples were collected from site with good ecological status (according to the WFD assessment approach) or characterized by a dominance of agricultural activities; they were subjected to little or no urban/industrial pressure, hence probably receiving much lower PFAS inputs. For samples exhibiting significant ΔPFCAs values, significant increases in C_4–C_{14} PFCA molar concentrations were observed (Table S11). The TOP assay method used in this work led to the formation of a series of PFCAs of different chain lengths and favored the production of short-chain PFCAs in comparison to other methods (Houtz and Sedlak 2012; Simonnet-Laprade et al. 2019); thus, the chain length profiles of unattributed pre-PFAAs could not be directly inferred from the PFCA pattern observed upon oxidation. However, our results provided evidence that unattributed precursors bearing perfluoroalkyl chains with up to 14 (and possibly more) fluorinated carbon atoms were buried in the analyzed sediments. This is consistent with the stronger sorption affinity of long-chain PFAS for this matrix (Labadie and Chevreuil 2011; Chen et al. 2020). Similar observations were previously made in a single urban river near Paris (France), *i.e.* significant formation of C_4–C_{12} PFCAs upon oxidation of sediment extracts (Simonnet-Laprade et al. 2019). The present study confirms such results and our findings suggest the widespread occurrence of long-chain PFAAs in sediments.

After oxidation, the molar fraction of $\sum$pre-PFAAs$_{unattributed}$ could be estimated based on the molar concentrations of $\sum$PFCAs, $\sum$PFSAs and $\sum$pre-PFAAs$_{targeted}$ determined through targeted analysis (Houtz et al. 2016; Simonnet-Laprade et al. 2019). The molar fraction of $\sum$pre-PFAAs$_{unattributed}$ was highly variable across samples and accounted on average for 51 ± 30 % of $\sum$PFAS (Figure S6). A handful of studies have previously reported on the quantification of unattributed precursors with the TOP assay

in sediments, albeit at limited spatial scale (Simonnet-Laprade et al. 2019; Meng et al. 2021). Here, we provided data that revealed the occurrence of a large but also variable fraction of unattributed pre-PFAAs in sediments at a nationwide scale. These values represented a low estimate of the extractable pre-PFAAs pool, as C_2–C_3 PFCAs may account for a large fraction of ΔPFCAs, depending on unattributed precursor structure and oxidation pattern (Meng et al. 2021). The oxidation of FTABs explained on average 4.3 ± 8.2 % of ΔPFCAs (up to 35 %), illustrating once again the necessity to broaden the scope of targeted PFAS using suitable sample preparation and quantification procedures.

3.4.2. Spatial distribution of pre-PFAAs

∑pre-PFAAs$_{unattributed}$ were positively correlated with ∑PFAS$_{targeted}$ (Figure 3) (slope = 1.02, Kendall's τ = 0.49, p < 0.001), even when excluding site St0112 from cluster#03 that presented the highest values (*i.e.* slope = 0.84, τ = 0.46, p < 0.001). Therefore, sampling sites with high levels of PFAS appeared more susceptible to present higher levels of unattributed precursors. These results are consistent with studies that investigated the spatial distribution of targeted and unattributed PFAS in water and sediments using high-resolution mass spectrometry, TOP assay or fluorine mass balance (Ye et al. 2014; D'Agostino and Mabury 2017; Chen et al. 2020).

Clusters determined from the HAC (Figure 2) were reported on Figure 3. Significant differences of ∑pre-PFAAs$_{unattributed}$ between clusters were found (p < 0.01). Sites from Cluster#01 presented low levels of unattributed precursors, contributing for 33 ± 35 % (mean ± standard deviation) to ∑PFAS (Table S12), supporting the prevalence of diffuse PFAS inputs at these sites. The contribution of ∑pre-PFAAs$_{unattributed}$ to ∑PFAS was the highest on average (64 ± 22 % of ∑PFAS) for Cluster#04; for this group of sites, levels of unattributed pre-PFAAs were usually elevated and higher than those of targeted PFAS, which is probably associated with industrial point sources (Glüge et al. 2020). Cluster#02 (St0516) and Cluster#03 generally displayed ∑PFAS similar to or higher than ∑pre-PFAAs$_{unattributed}$; the latter contributed for 48 ± 22% on average to ∑PFAS for these clusters. These sites presented the largest

fraction of $\sum\text{pre-PFAAs}_{targeted}$ (22 ± 20 % on average) (Table S13), most of which could be attributed to FTABs (up to 29%). Hence, these results further suggest that the $\sum\text{FTABs}$ / $\sum\text{PFAS}$ ratio could be a good indicator to identify sites under the influence of point source emissions linked to airport activities (Xiao 2017).

In any case, we showed at large spatial scale that, when elevated $\sum\text{PFAS}$ levels were quantified (*i.e.* > 1 ng g^{-1}), large fractions of unattributed pre-PFAAs could be expected, especially near urban and industrial areas.
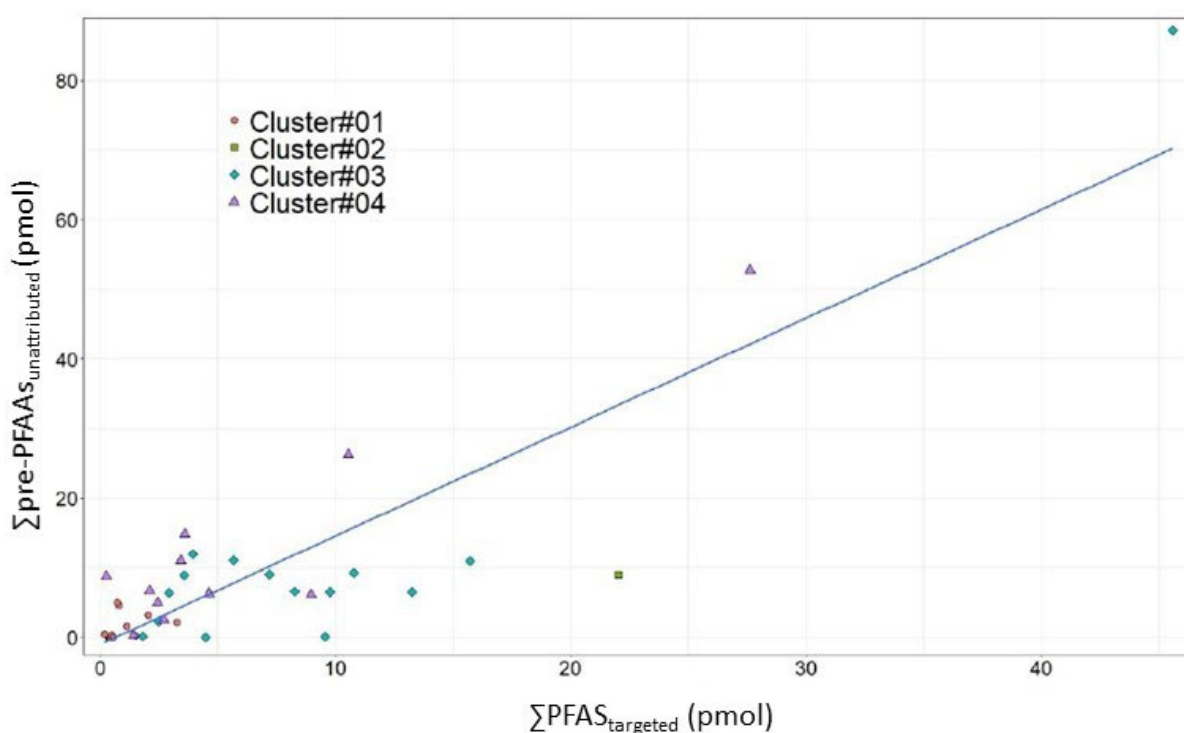

Figure 3. Correlation between $\sum\text{pre-PFAAs}_{unattributed}$ and $\sum\text{PFAS}_{targeted}$ in sediments. Sites are color-coded to reflect their attribution to clusters #01–#04 as previously determined through HAC (based on targeted analysis).

4. Conclusion

This study examined the occurrence and spatial distribution of targeted and unattributed PFAS in sediments at large spatial scale (*i.e.* French hydrographic network), through a combination of targeted analysis and TOP assay. Thanks to the improvement of the extraction procedure, the scope of these procedures was broadened to include zwitterionic PFAS, along with anionic and neutral ones. The developed TOP assay procedure provided an original approach for the estimation of extractable ∑pre-PFAAs_{unattributed} in sediments. While L-PFOS remained the major PFAS, several emerging compounds such as 6:2 FTAB, 8:2 FTAB or transformation intermediates (*e.g.* 5:3 FTCA) were also widely detected. These compounds significantly contributed to ∑PFAS, thereby confirming the need to extend the range of routinely targeted PFAS. Clustering analysis provided evidence for distinct molecular patterns that were further linked to urban or industrial activities. The TOP assay revealed the occurrence of substantial proportion of unattributed pre-PFAAs in sediments identified as impacted by PFAS point sources, which may be considered as a secondary source of PFAAs in hydrosystems. Thus, these results advocate for the need to use complementary approaches when analyzing PFAS in the aquatic environment; they also highlight the necessity to identify the structure of unattributed precursors (*e.g.* by suspect screening or non-target screening based on high-resolution mass spectrometry).

References

Ahrens, L., 2011. Polyfluoroalkyl compounds in the aquatic environment: a review of their occurrence and fate. *J. Environ. Monit.* **13**, 20–31. https://doi.org/10.1039/C0EM00373E

Ali, A.M., Sanden, M., Higgins, C.P., Hale, S.E., Alarif, W.M., Al-Lihaibi, S.S., Ræder, E.M., Langberg, H.A., Kallenborn, R., 2021. Legacy and emerging per- and polyfluorinated alkyl substances (PFASs) in sediment and edible fish from the Eastern Red Sea. *Environmental Pollution* **280**, 116935. https://doi.org/10.1016/j.envpol.2021.116935

Barzen-Hanson, K.A., Davis, S.E., Kleber, M., Field, J.A., 2017. Sorption of Fluorotelomer Sulfonates, Fluorotelomer Sulfonamido Betaines, and a Fluorotelomer Sulfonamido Amine in National Foam Aqueous Film-Forming Foam to Soil. *Environmental Science & Technology* **51**, 12394–12404. https://doi.org/10.1021/acs.est.7b03452

Boiteux, V., Bach, C., Sagres, V., Hemard, J., Colin, A., Rosin, C., Munoz, J.-F., Dauchy, X., 2016. Analysis of 29 per- and polyfluorinated compounds in water, sediment, soil and sludge by liquid chromatography–tandem mass spectrometry. *International Journal of Environmental Analytical Chemistry* **96**, 705–728. https://doi.org/10.1080/03067319.2016.1196683

Boiteux, V., Dauchy, X., Bach, C., Colin, A., Hemard, J., Sagres, V., Rosin, C., Munoz, J.-F., 2017. Concentrations and patterns of perfluoroalkyl and polyfluoroalkyl substances in a river and three drinking water treatment plants near and far from a major production source. *Science of The Total Environment* **583**, 393–400. https://doi.org/10.1016/j.scitotenv.2017.01.079

Buck, R.C., Franklin, J., Berger, U., Conder, J.M., Cousins, I.T., de Voogt, P., Jensen, A.A., Kannan, K., Mabury, S.A., van Leeuwen, S.P., 2011. Perfluoroalkyl and polyfluoroalkyl substances in the environment: Terminology, classification, and origins. *Integrated Environmental Assessment and Management* **7**, 513–541. https://doi.org/10.1002/ieam.258

Butt, C.M., Muir, D.C.G., Mabury, S.A., 2014. Biotransformation pathways of fluorotelomer-based polyfluoroalkyl substances: A review. *Environmental Toxicology and Chemistry* **33**, 243–267. https://doi.org/10.1002/etc.2407

Casson, R., Chiang, S.-Y.D., 2018. Integrating total oxidizable precursor assay data to evaluate fate and transport of PFASs. *Remediation Journal* **28**, 71–87. https://doi.org/10.1002/rem.21551

Chen, H., Munoz, G., Duy, S.V., Zhang, L., Yao, Y., Zhao, Z., Yi, L., Liu, M., Sun, H., Liu, J., Sauvé, S., 2020. Occurrence and Distribution of Per- and Polyfluoroalkyl Substances in Tianjin, China: The Contribution of Emerging and Unknown Analogues. *Environ. Sci. Technol.* **54**, 14254–14264. https://doi.org/10.1021/acs.est.0c00934

Cousins, I.T., DeWitt, J.C., Glüge, J., Goldenman, G., Herzke, D., Lohmann, R., Miller, M., Ng, C.A., Scheringer, M., Vierke, L., Wang, Z., 2020. Strategies for grouping per- and polyfluoroalkyl substances (PFAS) to protect human and environmental health. *Environ. Sci.: Processes Impacts* **22**, 1444–1460. https://doi.org/10.1039/D0EM00147C

D'Agostino, L.A., Mabury, S.A., 2017. Aerobic biodegradation of 2 fluorotelomer sulfonamide-based aqueous film-forming foam components produces perfluoroalkyl carboxylates: Biodegradation of 2 fluorotelomer sulfonamide surfactants. *Environ Toxicol Chem* **36**, 2012–2021. https://doi.org/10.1002/etc.3750

Dauchy, X., Boiteux, V., Bach, C., Rosin, C., Munoz, J.-F., 2017. Per- and polyfluoroalkyl substances in firefighting foam concentrates and water samples collected near sites impacted by the use of these foams. *Chemosphere* **183**, 53–61. https://doi.org/10.1016/j.chemosphere.2017.05.056

De Silva, A.O., Spencer, C., Scott, B.F., Backus, S., Muir, D.C.G., 2011. Detection of a Cyclic Perfluorinated Acid, Perfluoroethylcyclohexane Sulfonate, in the Great Lakes of North America. *Environ. Sci. Technol.* **45**, 8060–8066. https://doi.org/10.1021/es200135c

European Commission, 2013. Directive 2013/39/EU of the European Parliament and of the Council of 12 August 2013 amending Directives 2000/60/EC and 2008/105/EC as regards priority substances in the field of water policyText with EEA relevance 17.

European Commission, 2000. Directive 2000/60/EC of the European Parliament and of the Council of 23 October 2000 establishing a framework for Community action in the field of water policy [WWW Document]. URL https://eur-lex.europa.eu/resource.html?uri=cellar:5c835afb-2ec6-4577-bdf8-756d3d694eeb.0004.02/DOC_1&format=PDF (accessed 11.8.22).

Glüge, J., Scheringer, M., Cousins, I.T., DeWitt, J.C., Goldenman, G., Herzke, D., Lohmann, R., Ng, C.A., Trier, X., Wang, Z., 2020. An overview of the uses of per- and polyfluoroalkyl substances (PFAS). *Environ. Sci.: Processes Impacts* **22**, 2345–2373. https://doi.org/10.1039/D0EM00291G

Göckener, B., Eichhorn, M., Lämmer, R., Kotthoff, M., Kowalczyk, J., Numata, J., Schafft, H., Lahrssen-Wiederholt, M., Bücking, M., 2020. Transfer of Per- and Polyfluoroalkyl Substances (PFAS) from Feed into the Eggs of Laying Hens. Part 1: Analytical Results Including a Modified Total Oxidizable Precursor Assay. *J. Agric. Food Chem.* **68**, 12527–12538. https://doi.org/10.1021/acs.jafc.0c04456

Göckener, B., Fliedner, A., Rüdel, H., Badry, A., Koschorreck, J., 2022. Long-Term Trends of Per- and Polyfluoroalkyl Substances (PFAS) in Suspended Particular Matter from German Rivers Using the Direct Total Oxidizable Precursor (dTOP) Assay. *Environ. Sci. Technol.* **56**, 208–217. https://doi.org/10.1021/acs.est.1c04165

Guckert, M., Scheurer, M., Schaffer, M., Reemtsma, T., Nödler, K., 2022. Combining target analysis with sum parameters—a comprehensive approach to determine sediment contamination with PFAS and further fluorinated substances. *Environ Sci Pollut Res* **29**, 85802–85814. https://doi.org/10.1007/s11356-022-21588-x

Helsel, D.R., 2011. Statistics for Censored Environmental Data Using Minitab and R. John Wiley & Sons.

Hloušková, V., Lanková, D., Kalachová, K., Hrádková, P., Poustka, J., Hajšlová, J., Pulkrabová, J., 2014. Brominated flame retardants and perfluoroalkyl substances in sediments from the Czech aquatic ecosystem. *Science of The Total Environment* **470–471**, 407–416. https://doi.org/10.1016/j.scitotenv.2013.09.074

Houde, M., De Silva, A.O., Muir, D.C.G., Letcher, R.J., 2011. Monitoring of Perfluorinated Compounds in Aquatic Biota: An Updated Review: PFCs in Aquatic Biota. *Environmental Science & Technology* **45**, 7962–7973. https://doi.org/10.1021/es104326w

Houtz, E.F., Higgins, C.P., Field, J.A., Sedlak, D.L., 2013. Persistence of Perfluoroalkyl Acid Precursors in AFFF-Impacted Groundwater and Soil. *Environmental Science & Technology* **47**, 8187–8195. https://doi.org/10.1021/es4018877

Houtz, E.F., Sedlak, D.L., 2012. Oxidative Conversion as a Means of Detecting Precursors to Perfluoroalkyl Acids in Urban Runoff. *Environmental Science & Technology* **46**, 9342–9349. https://doi.org/10.1021/es302274g

Houtz, E.F., Sutton, R., Park, J.-S., Sedlak, M., 2016. Poly- and perfluoroalkyl substances in wastewater: Significance of unknown precursors, manufacturing shifts, and likely AFFF impacts. *Water Research* **95**, 142–149. https://doi.org/10.1016/j.watres.2016.02.055

Janda, J., Nödler, K., Scheurer, M., Happel, O., Nürenberg, G., Zwiener, C., Lange, F.T., 2019. Closing the gap – inclusion of ultrashort-chain perfluoroalkyl carboxylic acids in the total oxidizable precursor (TOP) assay protocol. *Environ. Sci.: Processes Impacts* 10.1039.C9EM00169G. https://doi.org/10.1039/C9EM00169G

Labadie, P., Chevreuil, M., 2011. Partitioning behaviour of perfluorinated alkyl contaminants between water, sediment and fish in the Orge River (nearby Paris, France). *Environmental Pollution* **159**, 391–397. https://doi.org/10.1016/j.envpol.2010.10.039

Liu, J., Mejia Avendaño, S., 2013. Microbial degradation of polyfluoroalkyl chemicals in the environment: A review. *Environment International* **61**, 98–114. https://doi.org/10.1016/j.envint.2013.08.022

Liu, M., Munoz, G., Vo Duy, S., Sauvé, S., Liu, J., 2022. Per- and Polyfluoroalkyl Substances in Contaminated Soil and Groundwater at Airports: A Canadian Case Study. *Environ. Sci. Technol.* **56**, 885–895. https://doi.org/10.1021/acs.est.1c04798

Liu, Z., Bentel, M.J., Yu, Y., Ren, C., Gao, J., Pulikkal, V.F., Sun, M., Men, Y., Liu, J., 2021. Near-Quantitative Defluorination of Perfluorinated and Fluorotelomer Carboxylates and Sulfonates with Integrated Oxidation and Reduction. *Environ. Sci. Technol.* **55**, 7052–7062. https://doi.org/10.1021/acs.est.1c00353

Martin, D., Munoz, G., Mejia-Avendaño, S., Duy, S.V., Yao, Y., Volchek, K., Brown, C.E., Liu, J., Sauvé, S., 2019. Zwitterionic, cationic, and anionic perfluoroalkyl and polyfluoroalkyl substances integrated into total oxidizable precursor assay of contaminated groundwater. *Talanta* **195**, 533–542. https://doi.org/10.1016/j.talanta.2018.11.093

Meng, Y., Yao, Y., Chen, H., Li, Q., Sun, H., 2021. Legacy and emerging per- and polyfluoroalkyl substances (PFASs) in Dagang Oilfield: Multimedia distribution and contributions of unknown precursors. *Journal of Hazardous Materials* **412**, 125177. https://doi.org/10.1016/j.jhazmat.2021.125177

Munoz, G., Desrosiers, M., Duy, S.V., Labadie, P., Budzinski, H., Liu, J., Sauvé, S., 2017. Environmental Occurrence of Perfluoroalkyl Acids and Novel Fluorotelomer Surfactants in the Freshwater Fish *Catostomus commersonii* and Sediments Following Firefighting Foam Deployment at the Lac-Mégantic Railway Accident. *Environ. Sci. Technol.* **51**, 1231–1240. https://doi.org/10.1021/acs.est.6b05432

Munoz, G., Duy, S.V., Labadie, P., Botta, F., Budzinski, H., Lestremau, F., Liu, J., Sauvé, S., 2016. Analysis of zwitterionic, cationic, and anionic poly- and perfluoroalkyl surfactants in sediments by liquid chromatography polarity-switching electrospray ionization coupled to high resolution mass spectrometry. *Talanta* **152**, 447–456. https://doi.org/10.1016/j.talanta.2016.02.021

Munoz, G., Giraudel, J.-L., Botta, F., Lestremau, F., Dévier, M.-H., Budzinski, H., Labadie, P., 2015. Spatial distribution and partitioning behavior of selected poly- and perfluoroalkyl substances in freshwater ecosystems: A French nationwide survey. *Science of The Total Environment* **517**, 48–56. https://doi.org/10.1016/j.scitotenv.2015.02.043

Munoz, G., Liu, J., Vo Duy, S., Sauvé, S., 2019. Analysis of F-53B, Gen-X, ADONA, and emerging fluoroalkylether substances in environmental and biomonitoring samples: A review. *Trends in Environmental Analytical Chemistry* e00066. https://doi.org/10.1016/j.teac.2019.e00066

Munoz, G., Ray, P., Mejia-Avendaño, S., Vo Duy, S., Tien Do, D., Liu, J., Sauvé, S., 2018. Optimization of extraction methods for comprehensive profiling of perfluoroalkyl and polyfluoroalkyl substances in firefighting foam impacted soils. *Analytica Chimica Acta* **1034**, 74–84. https://doi.org/10.1016/j.aca.2018.06.046

Pan, Y., Zhang, H., Cui, Q., Sheng, N., Yeung, L.W.Y., Sun, Y., Guo, Y., Dai, J., 2018. Worldwide Distribution of Novel Perfluoroether Carboxylic and Sulfonic Acids in Surface Water. *Environ. Sci. Technol.* **52**, 7621–7629. https://doi.org/10.1021/acs.est.8b00829

Pignotti, E., Casas, G., Llorca, M., Tellbüscher, A., Almeida, D., Dinelli, E., Farré, M., Barceló, D., 2017. Seasonal variations in the occurrence of perfluoroalkyl substances in water, sediment and fish samples from Ebro Delta (Catalonia, Spain). *Science of The Total Environment* **607–608**, 933–943. https://doi.org/10.1016/j.scitotenv.2017.07.025

Place, B.J., Field, J.A., 2012. Identification of Novel Fluorochemicals in Aqueous Film-Forming Foams Used by the US Military. *Environ. Sci. Technol.* **46**, 7120–7127. https://doi.org/10.1021/es301465n

Ruan, T., Jiang, G., 2017. Analytical methodology for identification of novel per- and polyfluoroalkyl substances in the environment. *TrAC Trends in Analytical Chemistry* **95**, 122–131. https://doi.org/10.1016/j.trac.2017.07.024

Shaw, D.M.J., Munoz, G., Bottos, E.M., Duy, S.V., Sauvé, S., Liu, J., Van Hamme, J.D., 2019. Degradation and defluorination of 6:2 fluorotelomer sulfonamidoalkyl betaine and 6:2 fluorotelomer sulfonate by Gordonia sp. strain NB4-1Y under sulfur-limiting conditions. *Science of The Total Environment* **647**, 690–698. https://doi.org/10.1016/j.scitotenv.2018.08.012

Simonnet-Laprade, C., Budzinski, H., Maciejewski, K., Le Menach, K., Santos, R., Alliot, F., Goutte, A., Labadie, P., 2019. Biomagnification of perfluoroalkyl acids (PFAAs) in the food web of an urban river: assessment of the trophic transfer of targeted and unknown precursors and implications. *Environ. Sci.: Processes Impacts* 10.1039.C9EM00322C. https://doi.org/10.1039/C9EM00322C

Wang, Z., Cousins, I.T., Scheringer, M., Hungerbühler, K., 2013. Fluorinated alternatives to long-chain perfluoroalkyl carboxylic acids (PFCAs), perfluoroalkane sulfonic acids (PFSAs) and their potential precursors. *Environment International* **60**, 242–248. https://doi.org/10.1016/j.envint.2013.08.021

Wang, Z., DeWitt, J.C., Higgins, C.P., Cousins, I.T., 2017. A Never-Ending Story of Per- and Polyfluoroalkyl Substances (PFASs)? *Environmental Science & Technology* **51**, 2508–2518. https://doi.org/10.1021/acs.est.6b04806

Xiao, F., 2017. Emerging poly- and perfluoroalkyl substances in the aquatic environment: A review of current literature. *Water Research* **124**, 482–495. https://doi.org/10.1016/j.watres.2017.07.024

Xiao, F., Jin, B., Golovko, S.A., Golovko, M.Y., Xing, B., 2019. Sorption and Desorption Mechanisms of Cationic and Zwitterionic Per- and Polyfluoroalkyl Substances in Natural Soils: Thermodynamics and Hysteresis. *Environ. Sci. Technol.* **53**, 11818–11827. https://doi.org/10.1021/acs.est.9b05379

Ye, F., Tokumura, M., Islam, M.S., Zushi, Y., Oh, J., Masunaga, S., 2014. Spatial distribution and importance of potential perfluoroalkyl acid precursors in urban rivers and sewage treatment plant effluent – Case study of Tama River, Japan. *Water Research* **67**, 77–85. https://doi.org/10.1016/j.watres.2014.09.014

Yeung, L.W.Y., De Silva, A.O., Loi, E.I.H., Marvin, C.H., Taniyasu, S., Yamashita, N., Mabury, S.A., Muir, D.C.G., Lam, P.K.S., 2013. Perfluoroalkyl substances and extractable organic fluorine in surface sediments and cores from Lake Ontario. *Environment International* **59**, 389–397. https://doi.org/10.1016/j.envint.2013.06.026

Zareitalabad, P., Siemens, J., Hamer, M., Amelung, W., 2013. Perfluorooctanoic acid (PFOA) and perfluorooctanesulfonic acid (PFOS) in surface waters, sediments, soils and wastewater – A review on concentrations and distribution coefficients. *Chemosphere* **91**, 725–732. https://doi.org/10.1016/j.chemosphere.2013.02.024

Zhang, S., Lu, X., Wang, N., Buck, R.C., 2016. Biotransformation potential of 6:2 fluorotelomer sulfonate (6:2 FTSA) in aerobic and anaerobic sediment. *Chemosphere* **154**, 224–230. https://doi.org/10.1016/j.chemosphere.2016.03.062